APEM journal
Advances in Production Engineering & Management 6 (2011) 3, 163-172
ISSN 1854-6250 Scientific paper

PRODUCTION & EVALUATION OF PCL SCAFFOLDS FOR TISSUE ENGINEERED HEART VALVES

Ragaert, K.*,**; De Somer, F.***; De Baere, I.**; Cardon, L.*,** & Degrieck, J.**
*CPMT group, Department of Applied Engineering Sciences, University College Ghent, Voskenslaan 362, B-9000 Ghent
**Department of Materials Science & Engineering, Ghent University, Technologiepark 903, B-9052 Ghent
***University Hospital Ghent, Heart Center 5IE-K12, De Pintelaan 185, B-9000 Ghent
E-mail: kim.ragaert@hogent.be

Abstract:
This research pertains to the suitability of thin 3D plotted poly-ε-caprolactone (PCL) leaflets as scaffolds for tissue engineering of aortic heart valve leaflets. More specifically, reproducibility of the production process and mechanical functionality of the synthetic leaflets were investigated. Multiple series of PCL leaflet scaffolds were manufactured with a BioScaffolder 3D plotting device. Both natural porcine leaflets and scaffolds were tested in an uni-axial burst experiment, indenting them with a ball-load until break. Maximum load, extension at break and a stiffness factor were calculated and the results compared. Scaffold geometry proved to be highly regular and reproducible. Variation in mechanical properties was noted for changing filament size. For some series it was possible to approximate the mechanical properties of the natural porcine leaflets with the plotted PCL leaflets.

Key Words: 3D Plotting, Scaffolds, PCL, Heart Valves

1. INTRODUCTION

Tissue Engineering is an advanced biomedical research field that looks to meet the growing demand for donor organs and tissues [1, 2]. According to the tissue engineering principle, biodegradable scaffolds are used as support structures for the culture of the patient's harvested cells in an in vitro environment, so as to (re)create healthy tissues meant to replace diseased ones. While this neo-tissue grows, the scaffold slowly degrades into nontoxic components, eventually leaving only the new, functional and healthy tissue behind. This final construct can be implanted into the patient and will not solicit any rejection, because the cells used are the patient's own. When looking to cardiovascular application and more specifically leaflets for heart valve replacement, the elastic-mechanical properties of the scaffold are just as important as biodegradability and non-toxicity of the material. The leaflet must be strong enough to withstand the blood pressure and at the same time be able to follow the elastic movement of a natural valve. When researching such valve scaffolds, we do not look for the strongest possible scaffold – as is the case with some other applications – but for the highest possible compliance with the elastic-mechanical behaviour of natural tissue. As such, the thermoplastic polyester poly-ε-caprolactone (PCL) makes a good material candidate [3, 4]. With its glass temperature well below zero, it is in the leathery state at both room and body temperature, which provides for a greater degree of elasticity when compared to the other well-known biocompatible polyesters like poly-(lactic acid) and poly-(glycolic acid).

In this research, 12 types of thin (0.43 to 1.24 mm) PCL scaffolds were created by 3D plotting and tested for their mechanical strength and stiffness. A comparison was made to the results of a series of natural porcine heart valve leaflets submitted to similar experiments.

We opt for a simple uni-axial burst experiment, which can be executed for the natural tissue as well as the easier-to-handle synthetic scaffolds. Although we are aware that uni-axial experiments do not suffice for a complete mechanical characterization of heart valve leaflets [5], it will give us an indication of the suitability of the tested scaffold geometries for use as heart valve leaflet. It is known to be remarkably difficult to determine a clear-cut set of mechanical properties for complicated anisotropic tissue like heart valve leaflets [6-9]. Composing a set of bulk material properties will not necessarily lead to a correct insight regarding the tissue's behaviour under load [9]. Ample research has been conducted on substitutive models [5, 10-13] as well as elaborate analysis of the different stress and strain components within the heart valve [9, 14-16]. Our goal however is not so much complete characterization as it is to establish the compliance of the PCL scaffolds to the load response of the natural valve leaflet. This functional behaviour largely determines the suitability of a scaffold [3, 8, 17].

2. EXPERIMENTAL

2.1 Natural leaflets

Fresh porcine hearts were obtained from the slaughterhouse. The aortic valve leaflets were excised and conserved in saline solution till testing. The time period between excision and testing was maximal 24 hrs. Leaflet position (left, right or non coronary) was noted for every sample. The left coronary (LC) and right coronary (RC) group both included 7 samples, while the non- coronary (NC) group included 6 samples. Rupture strength of the valve leaflets was tested with a Lloyd LF Plus Universal material tester. Before the test the valve leaflet was mounted over a round hole with the diameter 6.1 mm. Subsequently, a ball probe with a diameter of 4.45 mm approached the centre of the hole at a speed of 25 mm/min till perforation, which was defined as a sudden decrease in load with 50%. Force and displacement of the ball probe were recorded and used for calculation of maximum load at break (ML), extension at break (EXT) and the stiffness parameter (ST).

2.2 Scaffold material & production

Scaffolds material was PCL CAPA 6500 from Perstorp with number averaged molecular mass of 50000 Da and a melt temperature of 60°C [18].

All leaflets were manufactured by 3D plotting on a BioScaffolder machine (SysEng). The polymer was extruded at 110°C, on a 30°C plotting table. Spindle speed of the extrusion screw was constant at 200 rpm. The total of 12 scaffold series includes results from 6 different sizes of extrusion needles, resulting in different filament diameters FD. Two different orientation types for consecutive layers were used per FD: a relative layer orientation of 90° or 45°, resulting in scaffolds 0°/90°/0°/90° and 0°/45°/90°/-45° (further labelled as respectively 90- and 45-scaffolds for ease of reading). Speed of deposition F was adjusted per different extrusion needle to maintain regular filament and scaffold geometry. For each scaffold, strand distance SD was maintained at SD=1.8*FD and layer thickness LT was set at LT = FD-20µm. FD and SD are defined in Fig. 1 and an overview of the variable production parameters is given in Table I. Scaffolds are referred to per needle gauge and layer orientation (e.g. 25g90 scaffolds are made with 25 gauge needle and a 90° orientation between consecutive layers). Visual control of scaffolds was effected before and after loading with a Keyence 3D microscope VHX-500F.

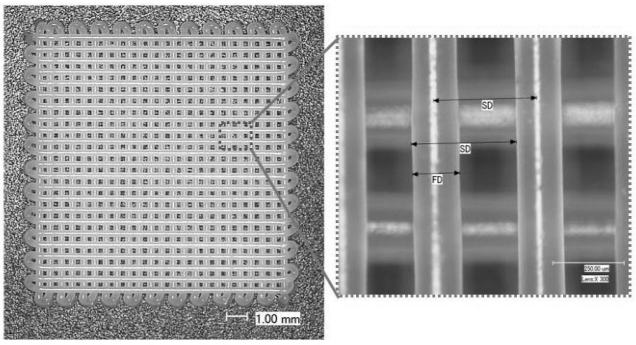

Figure 1: (left) High regularity of produced scaffolds and enlargement (right) for definition of filament diameter FD and strand distance SD.

Table I: processing parameters for the different scaffold series

needle	gauge	**22**	**23**	**25**	**27**	**28**	**31**
F	mm/min	200	200	160	120	80	220
FD	µm	410	330	250	200	180	127
LT	µm	390	310	230	180	160	107
SD	µm	738	600	450	360	324	230

2.4 Uni-axial testing of scaffolds

Scaffolds were tested on Lloyd LF Plus universal material tester according to a protocol similar to that applied to the natural leaflets. They were fixed over a round opening with diameter 11.07mm, and loaded until break with a spherical indenter (diameter 6.35mm) at a speed of 100mm/min. Force and displacement of the indenter probe were recorded and used for further determination of ML, EXT and ST. Per series, 3 scaffolds were tested and their results averaged.

2.5 Processing of results

Force-displacement results were transferred to Matlab 10 sotfware, with 500 measurement points per experiment, and smoothed with a 5-step progressive average filter. The curves were cut at a threshold value of F=0.1N (for natural leaflets) or F=0.3N (for PCL scaffolds), and at maximum load. Displacement of the probe was converted to extension (depth of indenting). ST parameter was calculated as the slope of the best-fitting linear curve in the linear area between 3 and 8N.

Statistical analysis was performed with SPSS16, through either a simple t-test or a one-way ANOVA test, both with p=0.05 significance level.

3. RESULTS

3.1 Natural leaflets

A summarized overview of the test results for the natural valve leaflets is given in Table II and visualized in Figure 2. The variation on the resulting values for EXT, ML and ST is within the expectations for natural tissue.

Table II: Summary of indentation testing results for natural heart valve leaflets.

position		EXT	ML	ST
LC	Mean	2,8820	16,7333	8,5539
	N	7	7	7
	Std. Deviation	,71129	3,93519	1,27614
RC	Mean	2,5073	15,4097	9,1223
	N	7	7	7
	Std. Deviation	,71753	2,75826	,87197
NC	Mean	2,3212	13,9335	8,6184
	N	6	6	6
	Std. Deviation	,37779	3,38953	,36986
Total	Mean	2,5826	15,4301	8,7722
	N	20	20	20
	Std. Deviation	,64544	3,41311	,92767

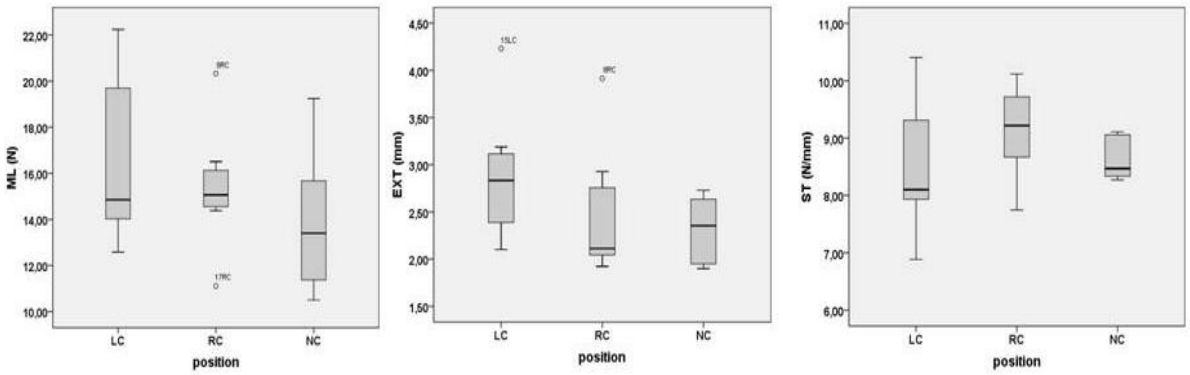

Figure 2: Results for uni-axial testing of natural valve leaflets, grouped per coronary position. From left to right: ML, EXT and ST.

Tested heart valve leaflets and their EXT, ML & ST values are categorized by coronary position. Reviewing the graphical comparison of results by these categories however, imposes the question whether this division is useful and relevant. Subsequent comparison of these result groups by one-way ANOVA reveals no significant difference in values of ML ($p=0.356$), EXT ($p=0.288$) or ST ($p=0.485$) between the three groups. Therefore, it is concluded that all valve leaflets can be pooled into one group and their results for uni-axial indentation summarized as follows (n=20): EXT = 2.58mm (± 0.64mm), ML = 15.43N (± 3.41N) and ST = 8.77 N/mm (± 0.93 N/mm).

3.2 Mechanical properties of PCL scaffolds

An overview of the results for the mechanical properties of PCL leaflets is given in Table III and illustrated by Figure 3 and Figure 4.

Table III: Overview of results for mechanical testing of PCL leaflets.

		ST		EXT		ML	
series	**FD**	**mean**	**stdev**	**mean**	**stdev**	**mean**	**stdev**
	µm	N/mm	N/mm	mm	mm	N	N
22g45	410	22,35	2,20	4,20	0,63	66,11	1,51
22g90	410	21,48	5,87	3,99	0,77	72,86	4,62
23g45	330	17,30	0,19	3,78	0,40	42,72	5,86
23g90	330	16,43	3,77	4,04	0,57	48,84	2,32
25g45	250	17,32	0,26	4,28	0,08	50,25	1,06
25g90	250	16,83	0,35	4,06	0,18	48,45	2,42
27g45	200	12,35	0,98	3,37	0,14	25,50	0,22
27g90	200	11,76	2,30	3,46	0,48	24,56	0,44
28g45	180	9,88	0,72	3,31	0,19	19,92	0,71
28g90	180	11,43	0,73	4,20	0,36	24,32	1,54
31g45	127	10,98	0,23	3,49	0,25	21,69	0,29
31g90	127	10,43	0,94	4,18	0,78	22,02	0,68

Conform to expectations, the scaffolds with smaller FD also exhibit lower values for ML. At first sight, there does not appear to be any difference between scaffolds from the 45- and 90-series of the same FD, yet t-test indicates a significant difference for the 27g (p= 0.046) and 28g (p=0.024) series. A remarkable result is that the scaffolds would seem to be divided into two classes, with high ML values for 22g to 25g and lower ML values for 27g to 31g.

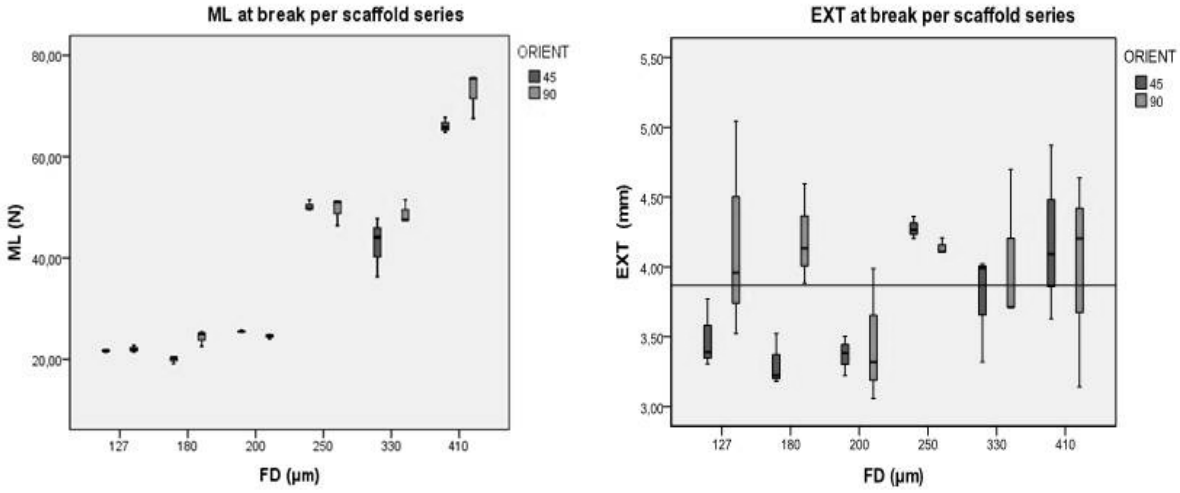

Figure 3: Maximum load ML (left) and extension at break EXT (right) for the different scaffold series. Overall mean EXT is indicated by horizontal line (EXT_{mean}=3.86 mm).

No defining trend is to be established for the value of EXT. Scaffold layer orientation and FD seem to have no influence on the extension at break, which is confirmed by statistics. There is no significant difference for varying FD within the 45 (ANOVA, p=0.063) or 90 group (ANOVA, p=0.796) , nor between the grouped results for 45 and 90 orientation (t-test, p=0.131).

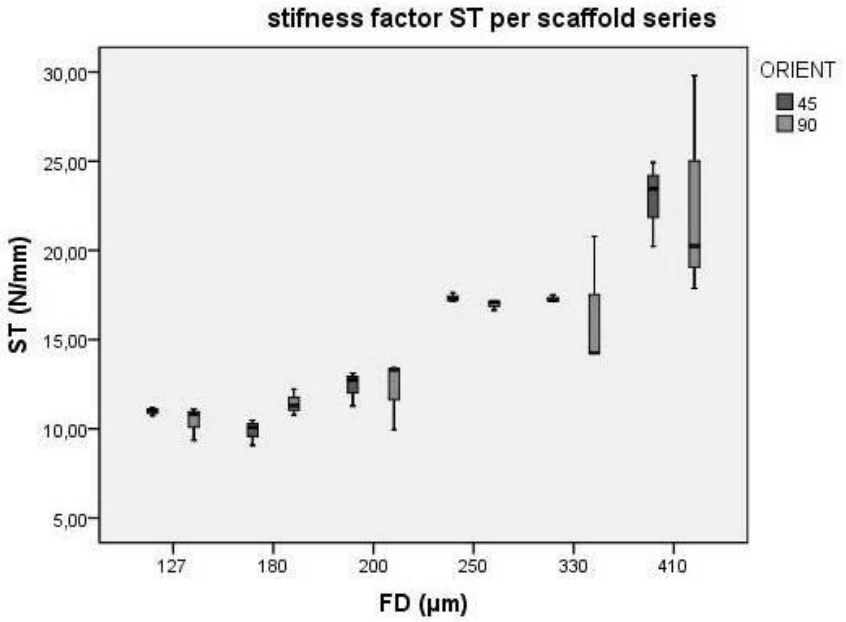

Figure 4: Stiffness factor ST for different scaffold series.

ST, the variable which is of greatest interest to us, displays a similar trend as ML. The ST value is lower for those scaffolds composed of thinner filaments. It is notable that if a larger variation on the ST results occurs, it is within the 90 orientation group. As with ML, graphic display of the results suggests that there would be two general classes of scaffolds, with higher ST values for the coarser scaffolds (22g to 25g) and lower ST values for the finer scaffolds (27g to 31g). Per separate FD group, there is no significant difference between the 45 and 90 scaffolds.

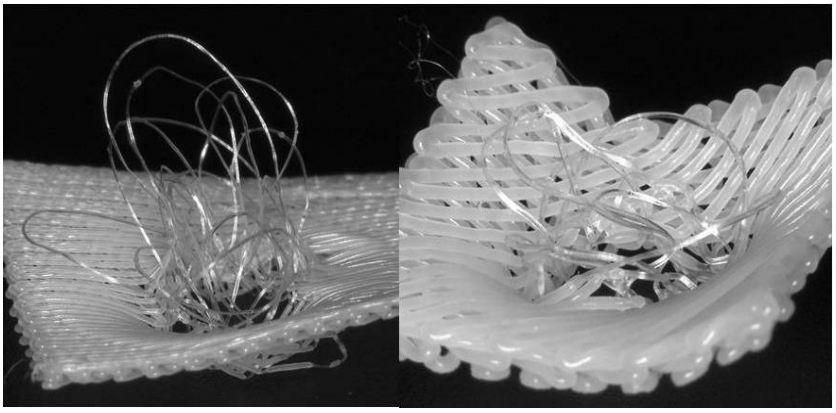

Figure 5: Individual PCL filaments are not broken but deformed during loading.

3.2 Visual control

Visual inspection revealed that the produced scaffolds possess a high degree of regularity in FD and SD, as illustrated in Figure 1. The chosen parameter sets result in regular and reproducible scaffolds. Additionally, filament layers did not delaminate during indentation. During loading, the individual filaments that make up the scaffolds are not actually broken. Instead, they are subject to a plastic deformation that elongates them up to the point where the indenter body can move between the filaments. This phenomenon is shown in Figure 5.

4. DISCUSSION

Whilst there is little difference in the total depth of indentation (EXT) prior to break for all scaffolds, a clear difference can be observed in the modus of deformation between the different layer orientation groups. Scaffolds with the 45 orientation systematically suffered less local deformation before the probe passed through. The visual inspection of the tested scaffolds reveals that the 45-scaffolds are more prone to bending in a saddle-like shape as opposed to the 90-scaffolds which evidence local craterlike deformation around the point of impact with the probe. This can be seen in Figure 6.

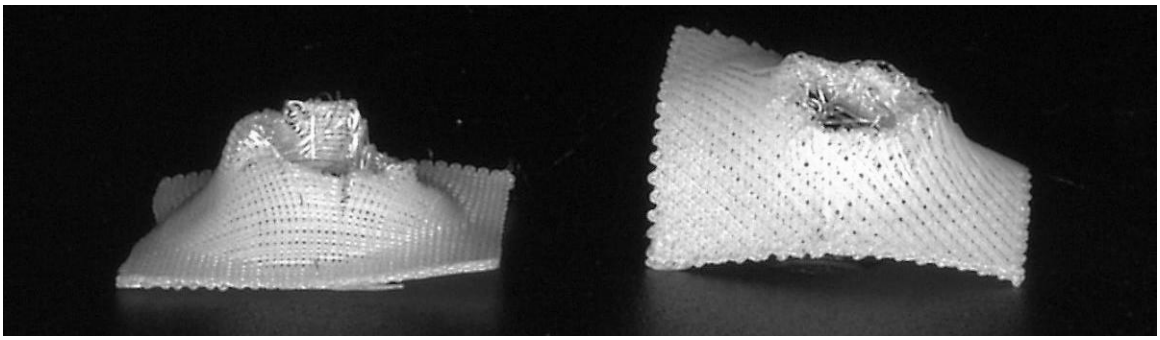

Figure 6: Different modus of deformation for 90- (left) and 45- (right) scaffolds.

An explanation can be found in that the 90-scaffolds exhibit more symmetry and are thus more likely to exhibit homogenous behaviour; with only four layers plotted, the 45-scaffolds are completely asymmetric. Plotting the 90-scaffolds for five layers (0/90/0/90/0 scaffold).would render them symmetric around the middle layer and as such fully eliminate the saddle effect.

There is a notably large amount of variation on the values for EXT. We attribute this to the lack of control on the point of first impact for the ball probe. Whether this contact point is located in a pore, on a filament or even an overlap point of two filaments, will influence the ball probe's ability to slip in between individual filaments as described earlier. This effect is stronger for the 90-scaffolds than for the 45-scaffolds as pores in the 90-scaffolds go all the way through, whilst the 45-scaffolds have supporting filaments above or under every pore. It equally accounts for larger variation on ST results within the 90-group as well as for the coarsest scaffolds, which have both the largest pores and the thickest individual filaments.

As stated during the introduction, we do not aim to obtain a maximal mechanical strength for the scaffolds but to approximate as closely as possible the behaviour under load of natural heart valve leaflets. In the natural position, heart valves are uniformly loaded with a fluid pressure and not by bullet indentation. We consider the ML and EXT to be no more than useful information, as these are derived from the moment of physical leaflet rupture. They refer more closely to the considerable strength of PCL fibres than to the flexibility of the scaffold. It is the stiffness parameter ST which has our main interest, it being an indication of the elastic response under physiological loading.

Based on the results of ML and ST, we can divide the tested scaffold series into two so-called stiffness classes: the higher class comprises the scaffolds of the 22g to 25g series (FD = 410-250 µm), and the lower class the scaffolds of the 27g to 31g series (FD = 200-127 µm). Statistical analysis through independent t-test reveals clear significant difference between the two classes (p=0,000 for both ST and ML). The thicker filaments making up the parts from the high stiffness class offer too much individual strength to allow for the necessary flexibility to approximate the behaviour of the natural leaflets, leading to high values of ML and ST. We therefore discard them for use as a valve scaffold.

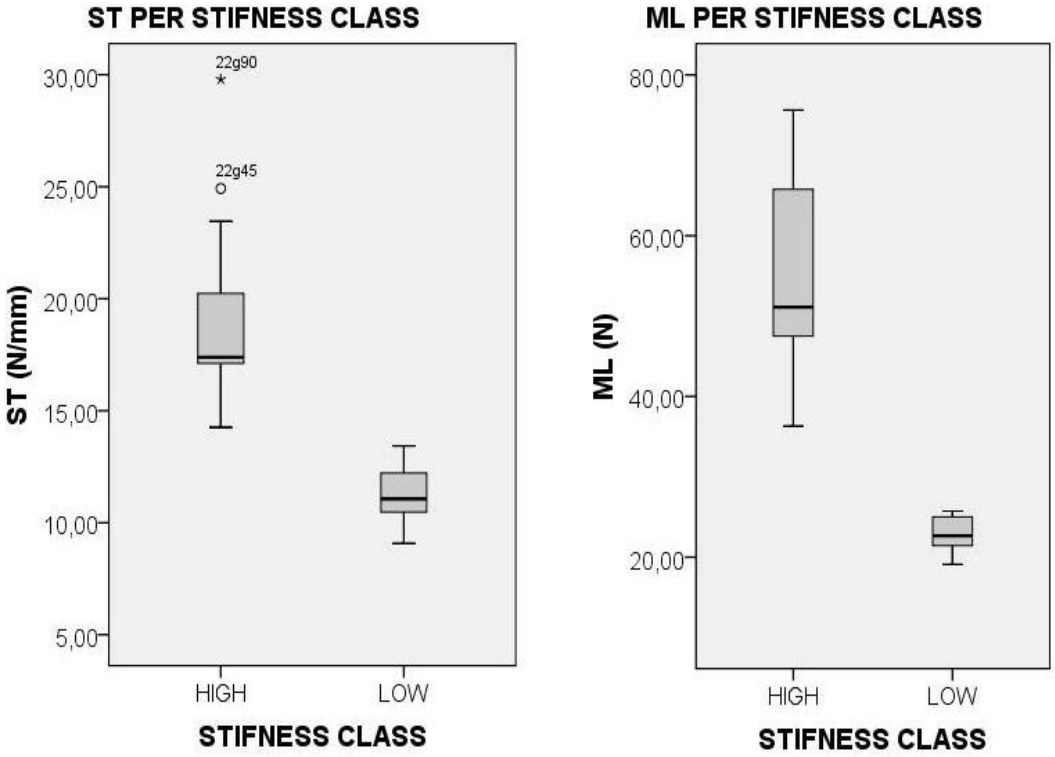

Figure 1: ST and ML for scaffolds groups per stiffness class.

Scaffolds from the lower stiffness class are made up of finer extruded filaments; the individual filament is thinner and the alternation rate material/porosity is higher, allowing for a clearly more flexible behaviour under load. These scaffolds, and more specifically the 28g and 31g series (mean ST values ranging from 9.88 to 11.43 N/mm) are nearing the range of the elastic response of natural leaflets (ST = 8.77 ± 0.93 N/mm). Even maximum strength ML is reduced to approach more nearly the results of natural valve leaflets (ML = 15.43N ± 3.41N), with values of roughly 20 to 25 N. As we include these scaffolds in further research to produce a PCL-based leaflet for heart valves, we must consider how to further enhance flexibility so that the load behaviour of the natural tissue may be simulated even more closely. One approach may be to increase the SD parameter in order to create a larger overall porosity. When doing so, one must take care however to maintain layer integrity and avoid collapse of the extruded filament into the underlying large pores. Alternatively it would be feasible to compound the PCL material with lower molecular weight fractions or even other biocompatible thermoplastics to decrease stiffness on the level of the polymer chains.

As the relative orientation of the extruded layers does not appear to affect ST parameter, it would be useful to continue research with 90-series, so that the scaffolds can be made symmetric in the height by working with an uneven amount of layers. Certainly a reduction from four to three layers of material would further improve suppleness of the scaffolds.

We would like to offer some closing thoughts on the clinical relevance of these results. The tested scaffolds were unmodified PCL and not seeded with cells. The presence of cells will most certainly affect the mechanical response of the construct to loading. Moreover, unmodified PCL is rather hydrophobic and as such not well-suited to cell attachment. Known techniques to enhance material attractiveness to cells include copolymerization [19], blending [20], and surface treatment [21, 22]. Our results indicate that the “base” material will be capable of a mechanical behaviour approximating to that of natural heart valve leaflets. It will be the subject of further research if suitably modified PCL materials will equally match these criteria and how they will perform under cyclic loading.

5. CONCLUSION

Production of PCL scaffolds by 3D plotting on BioScaffolder machine yields regular and reproducible parts for a varying range of filament sizes. Both natural heart valve leaflets and their synthetic counterparts were tested for response to load in an uni-axial burst experiment. Scaffolds with finer individual filaments (200 µm and less) showed good promise for the approximation of the low stiffness of the natural valves. Further research to improve this flexibility will include altering design parameters of the scaffold and modification of the base PCL material.

NOTES & ACKNOWLEDGEMENTS

This manuscript is an extended version of the paper “PCL leaflets for tissue engineered heart valves: 3D plotting and mechanical properties”, submitted at PMI 2010 conference. It contains an extra section on mechanical testing of the natural heart valve leaflets, extended discussion, added test results for scaffolds produced with a 22g needle and a retrial of the 27g series, which were found to delaminate in the first test series that was discussed in the conference paper.

The authors would like to extend their gratitude to dr. Pamela Somers for the excision and preparation of the natural heart valve leaflets. Scaffold production research is funded by the Department of Applied Engineering Sciences at University College Ghent.

REFERENCES

[1] Mikos, A.G. and J.S. Temenoff (2000). Formation of highly porous biodegrdable scaffolds for tissue engineering, Electronic Journal of Biotechnology, 3(2)

[2] Isenberg, B.C. and J.Y. Wong, Building structure into engineered tissues (2006). Materials Today, 9(12): p. 54-60

[3] Brody, S. and A. Pandit (2007). Approaches to heart valve tissue engineering scaffold design, Journal of Biomedical Materials Research Part B-Applied Biomaterials, 83B(1): p. 16-43.

[4] Filova, E., et al., Tissue-Engineered Heart Valves. Physiological Research, 2009. 58: p. S141-S158

[5] Cox, M.A.J., et al. (2008). Mechanical characterization of anisotropic planar biological soft tissues using finite indentation: Experimental feasibility, Journal of Biomechanics, 41(2): p. 422-429

[6] Sacks, M.S., W.D. Merryman, and D.E. Schmidt (2009). On the biomechanics of heart valve function, Journal of Biomechanics, 42(12): p. 1804-1824

[7] Sacks, M.S. and A.P. Yoganathan (2007). Heart valve function: a biomechanical perspective, Philosophical Transactions of the Royal Society B-Biological Sciences, 362(1484): p. 1369-1391

[8] Stella, J.A., et al. (2010). On the biomechanical function of scaffolds for engineering load-bearing soft tissues, Acta Biomaterialia, 6(7): p. 2365-2381

[9] Weinberg, E.J., D. Shahmirzadi, and M.R.K. Mofrad (2010). On the multiscale modeling of heart valve biomechanics in health and disease, Biomechanics and Modeling in Mechanobiology, 9(4): p. 373-387

[10] Fonck, E. (2007). Effect of elastin degradation on carotid wall mechanics as assessed by a constituent-based biomechanical model, American Journal of Physiology-Heart and Circulatory Physiology, in press

[11] Zulliger, M.A., et al. (2004). A strain energy function for arteries accounting for wall composition and structure, Journal of Biomechanics, 37(7): p. 989-1000

[12] Zulliger, M.A., A. Rachev, and N. Stergiopulos (2004). A constitutive formulation of arterial mechanics including vascular smooth muscle tone, American Journal of Physiology-Heart and Circulatory Physiology, 287(3): p. H1335-H1343

[13] Cox, M.A.J., et al. (2010). Tissue-Engineered Heart Valves Develop Native-like Collagen Fiber Architecture, Tissue Engineering Part A, 16(5): p. 1527-1537

[14] Labrosse, M.R., et al. (2006). Geometric modeling of functional trileaflet aortic valves: Development and clinical applications. Journal of Biomechanics, 39(14): p. 2665-2672
[15] Labrosse, M.R., K. Lobo, and C.J. Beller (2010). Structural analysis of the natural aortic valve in dynamics: From unpressurized to physiologically loaded, Journal of Biomechanics, 43(10): p. 1916-1922
[16] Kassab, G.S. (2006). Biomechanics of the cardiovascular system: the aorta as an illustratory example, Journal of the Royal Society Interface, 3(11): p. 719-740
[17] Sachlos, E., et al. (2003). Novel collagen scaffolds with predefined internal morphology made by solid freeform fabrication. Biomaterials, 24(8): p. 1487-1497
[18] Perstorp (2003). Capa 6000 series data sheet, P.U. Ltd, Editor
[19] Lemmouchi, Y., et al. (2007). Novel synthesis of biodegradable amphiphilic linear and star block copolymers based on poly(epsilon-caprolactone) and poly(ethylene glycol), Journal of Polymer Science Part a-Polymer Chemistry, 45(17): p. 3975-3985
[20] Wang, Z.W., et al. (2010). Preparation and Properties of Nano Calcium Deficient Apatite/Poly (epsilon-caprolactone) Composite Scaffold, Journal of Inorganic Materials, 25(5): p. 500-506
[21] Yildirim, E.D., et al. (2010). Accelerated differentiation of osteoblast cells on polycaprolactone scaffolds driven by a combined effect of protein coating and plasma modification, Biofabrication, 2(1)
[22] Yeo, A., W.J. Wong, and S.H. Teoh (2010). Surface modification of PCL-TCP scaffolds in rabbit calvaria defects: Evaluation of scaffold degradation profile, biomechanical properties and bone healing patterns, Journal of Biomedical Materials Research Part A, 93A(4): p. 1358-1367